Magnesium Technology 2011
Edited by: Wim H. Sillekens, Sean R. Agnew, Neale R. Neelameggham, and Suveen N. Mathaudhu
TMS (The Minerals, Metals & Materials Society), 2011

The microstructure and mechanical properties of cast Mg-5Sn based alloys

M. Keyvani, R. Mahmudi, G. Nayyeri

School of Metallurgical and Materials Engineering, University of Tehran, Tehran, Iran

Keywords: Mg-5Sn alloy; microstructure; creep resistance; mechanical properties.

Abstract

The effects of 1 wt.% Ce-rich misch-metal, 3 wt.% Bi, 0.4 wt.% Sb, and 2 wt.% Ca additions on the microstructure, mechanical properties, and creep resistance of a cast Mg-5Sn alloy were studied. Impression creep tests were carried out at 150 and 225 °C under constant stresses of 300 and 175 MPa. The results showed that creep resistance, hardness, and shear strength of the base alloy were significantly enhanced with the addition of ternary alloying elements. This was attributed to the concurrent formation of Mg_2Sn particles with the more thermally stable CaMgSn, Mg_3Sb_2, Mg_3Bi_2 and MgSnRE phases which strengthen both matrix and grain boundaries during deformation in the investigated system. Among all tested materials, the Mg-5Sn-2Ca alloy indicated the highest mechanical properties and creep resistance due to the refined microstructure as well as the type and volume fraction of the intermetallic phases present in this alloy.

Introduction

In recent years, research and development of magnesium alloys have been greatly promoted by the lightweight requirement in the automotive industry [1]. Despite their good combination of low density and high strength-to-density ratio, Mg alloys suffer from low mechanical properties at elevated temperatures [2]. Therefore, attempts have been made to develop new magnesium alloys having improved structural stability at the elevated temperatures. Among many possibilities, the Mg-Sn alloy system appears to be promising for high temperature applications. This is attributed to the formation of the thermally stable Mg_2Sn phase, which is mainly distributed along the grain boundaries in the as-cast condition [3,4].

The study of the microstructure, tensile properties, and creep resistance of cast Mg-Sn alloys by Liu et al. [5] has shown that the Mg-5Sn alloy exhibits the best combination of tensile properties at ambient temperature and a reasonable creep resistance at 150 °C. The compression [6] and impression [7] creep study of the Mg-5Sn alloy has indicated that the dispersive distribution of Mg_2Sn precipitates is the main cause of the enhanced creep resistance of the material. To further enhance the mechanical and creep properties of the Mg-Sn alloys, various alloying elements have been used. Nayyeri and Mahmudi reported that additions of Sb and Ca into the Mg-5Sn alloy significantly improved the creep resistance [8,9], hot hardness [10], and high temperature shear strength of the material [11]. Similar strength improvement has been observed after adding La [12], Di [13], and Bi [10] to the Mg-Sn alloys. The achieved enhancement in the strength and creep resistance has been attributed to the respective formation of the thermally stable Mg_3Sb_2, CaMgSn, MgSnRE, and Mg_3Bi_2 intermetallic particles, which strengthen both matrix and grain boundaries and oppose recovery and recrystallization processes during creep and deformation at elevated temperatures.

The aim of this study is to examine the effects of different alloying elements, such as RE, Bi, Sb, and Ca on the microstructure, creep properties, hardness, and shear strength of the Mg-5Sn alloy in the as-cast condition. The evaluation of strength is made by using the shear punch testing (SPT) technique, which has been attempted previously for evaluating the strength of some cast Mg alloys [14,15]. This is an efficient method that is capable of producing strength data which are well correlated with those found by the conventional tensile tests [16].

Experimental procedure

The five alloys designed for this investigation were based on Mg-5 wt.% Sn with 1%RE, 3%Bi, 0.4%Sb, and 2%Ca additions. High purity Mg, Sn, Bi, Sb, Ca, and a misch-metal composed of 50.6%Ce, 23.2%La, 20.3%Nd, and 5.9% Pr, were melted in an electrical furnace under a protective flux. The melts were held at 750 °C for 30 min and then poured into a steel die, preheated to 150 °C. To examine the microstructure of the materials, the specimens were studied by optical and scanning electron microscopy (SEM). For microstructural analysis, the polished samples were etched using a 5% nitric acid and 95% ethyl alcohol solution at room temperature. X-ray diffraction (XRD) analysis was carried out to identify the phases.

4-mm thick slices were tested in an impression tester. The details of impression testing arrangement are explained elsewhere [17] and will only be briefly described here. A SANTAM universal tensile testing machine equipped with a three-zone split furnace was used to perform constant-load impression tests. A flat ended cylindrical punch of 2 mm diameter was mounted in a holder which was positioned in the center of the vertical loading bar. The specimen was located on an anvil below the loading bar and the assembly of specimen and indenter was accommodated by the split furnace. Impression creep measurements were made at 150 and 225 °C and under respective punch stresses of 300 and 175 MPa. After application of the load, the impression depth was measured automatically as a function of time by the machine and the data were acquired by a computer.

The hardness of the alloys was measured in a Vickers hardness tester with an indenter load of 100 N and a loading time of 30 s. Each reading was an average of at least five separate measurements taken at random places on the surface of the specimens. The strength of the materials was assessed by the shear punch testing. The 1-mm thick slices were ground to a thickness of 0.6 mm, from which disks of 10 mm in diameter were punched for the SPT. A shear punch fixture with a 3.175 mm diameter flat cylindrical punch and 3.225 mm diameter receiving-hole was used for this experiment. Shear punch tests were performed at room temperature using a screw driven SANTAM material testing system with a load cell of 20 kN capacity and a

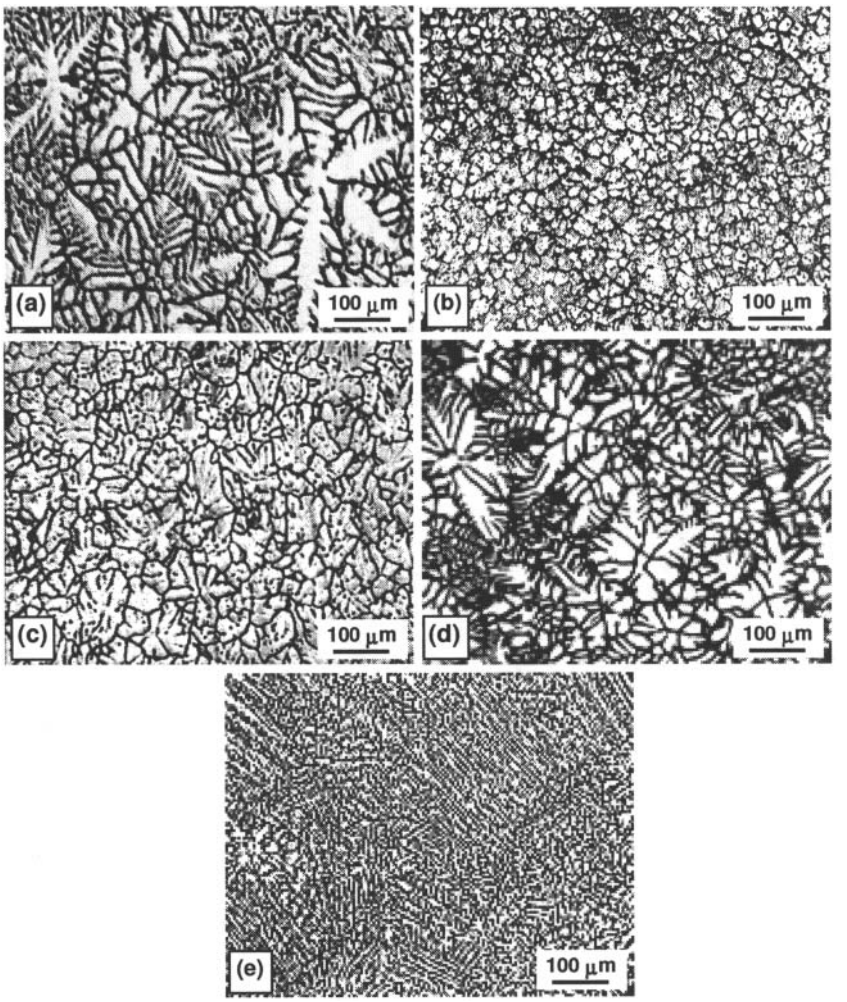

Fig. 1. Optical micrographs showing the as-cast dendritic structure of: (a) Mg-5Sn, (b) Mg-5Sn-2Ca, (c) Mg-5Sn-0.4Sb, (d) Mg-5Sn-3Bi, and (e) Mg-5Sn-1RE.

crosshead speed of 0.25 mm/min. After application of the load, the applied load P was measured automatically as a function of punch displacement; the data were acquired by a computer so as to determine the shear stress of the tested materials using the relationship:

$$\tau = \frac{P}{\pi dt} \qquad (1)$$

where P is the punch load, t is the specimen thickness and d is the average of the punch and die diameters. Three different samples were tested for each condition and it was observed that the variation in the measured ultimate shear strength values was small.

Results and discussion

The optical micrographs of the investigated alloys are depicted in Fig. 1. It can be observed that after addition of Bi, Sb, and Ca the coarse dendritic structure of the Mg-5Sn alloy is generally refined. The most pronounced refinement occurs at 2 wt.% Ca where it can be seen that the initial dendritic structure is broken and a rather uniform distribution of the microstructure constituents is achieved. RE addition decelerates the growth of secondary dendrites, but has little effect on grain refining. During the solidification process, enrichment of RE elements in solid-liquid interface induces the constitution undercooling at the solidification interface front, decreasing the secondary dendrites' growth.

The XRD patterns exhibited in Fig. 2 indicate that α-Mg and Mg_2Sn are the only constituents of the Mg-5Sn alloy. In the Bi-, Sb-, and Ca-bearing materials, additional diffraction peaks emerged, corresponding respectively to the Mg_3Bi_2, Mg_3Sb_2, and CaMgSn intermetallic compounds. For the RE-containing material, some new peaks were observed near 24.5, 42, and 49.5°. However, these diffraction peaks could not be identified by the XRD database. It is worth noting that the intensity of the Mg_2Sn peaks decreases in the ternary alloys.

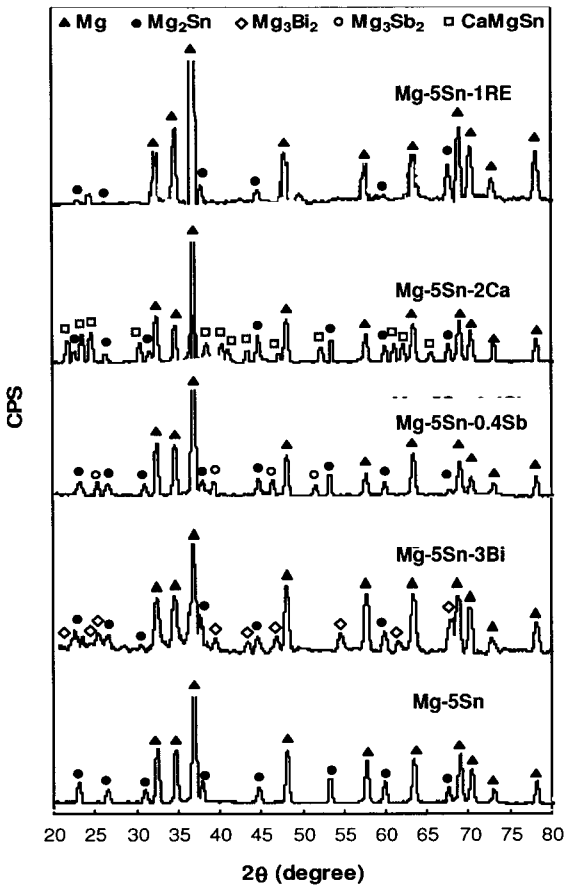

Fig. 2. XRD pattern of the investigated alloys.

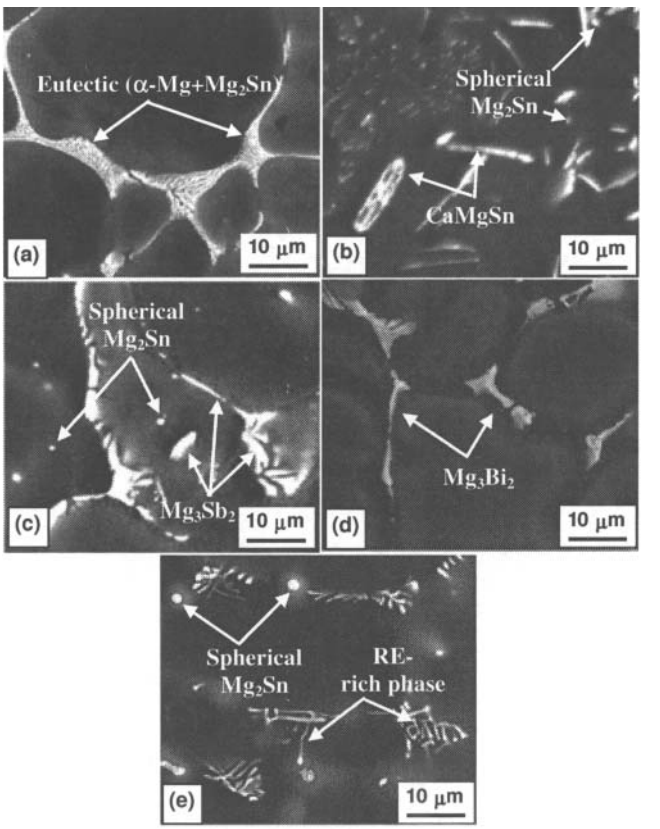

Fig. 3. SEM micrographs showing the distribution of the second phase particles in the α-Mg matrix for: (a) Mg-5Sn, (b) Mg-5Sn -2Ca, (c) Mg-5Sn-0.4Sb, (d) Mg-5Sn-3Bi, and (e) Mg-5Sn-1RE.

For a clearer view of the microstructure and phases present in the magnesium matrix, SEM images of all tested materials are shown in Fig. 3. The microstructure of the Mg-5Sn alloy is composed of the primary α-Mg matrix and the lamellar eutectic structure (α-Mg + Mg_2Sn) at the grain boundaries (Fig. 3a). In contrast to the microstructure of the base alloy, the α-Mg dendrites are refined and the intermetallic Mg_2Sn phase is present in the form of spherical particles in ternary alloys. In addition, a new rod-shaped phase can be detected mainly at the grain boundaries in Bi-, Sb-, and Ca-containing alloys. According to the XRD analysis, these intermetallic compounds should be Mg_3Bi_2, Mg_3Sb_2, and CaMgSn, respectively. These particles may have formed prior to the solidification of the Mg matrix, acting as powerful nucleation sites, the consequence of which is a refined microstructure [18]. In the Mg-5Sn-1RE alloy, however, some branch-like particles can be seen around the grain boundaries. These particles should be a RE-rich phase, the identification of which was not possible in the XRD pattern of the alloy.

Fig. 4 shows a comparison of impression creep curves under punching stresses of 300 MPa at 150 °C and 175 MPa at 225 °C. As can be seen, after a short primary creep stage almost all of the curves exhibit a relatively long steady-state region where depth increases linearly with time. Furthermore, it can be noticed from the level and slope of the curves that different materials demonstrate different creep behavior under both stress levels. According to this figure, third element addition into the Mg-5Sn alloy generally improves the creep resistance of the material, the effect which becomes more pronounced after Ca addition.

Fig. 5 exhibits the SPT data, presented as the variation of shear stress with normalized displacement obtained for all five alloys. It can be observed that, similar to conventional tensile stress-strain curves, after a linear elastic behavior the curves deviate from linearity before they reach a maximum point. The deviation point is taken as the shear yield stress (SYS) and the stress corresponding to the maximum point is referred to as the ultimate shear strength (USS). It is evident that all ternary alloys have higher USS values than the binary base alloy. In accordance with the creep results, the highest strength belongs to the Ca-containing alloy. To have a better comparison of the effect of alloying elements on the strength of the base material, the USS and SYS data are summarized in Fig. 6. The results indicate that addition of all alloying elements improves both shear and ultimate strength of the base Mg-5Sn alloy. Addition of Ca has the most pronounced effect, while RE addition exhibits the weakest effect. A similar trend is observed for the hardness of the alloys shown in Fig. 7.

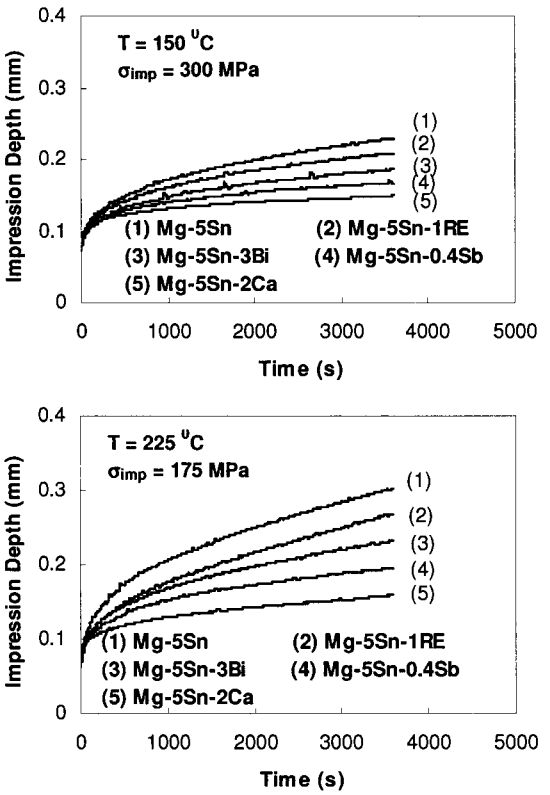

Fig. 4. Comparison of creep behavior of the investigated alloys at: a) T = 150 °C, σ_{imp} = 300 MPa, and b) T = 225 °C, σ_{imp} = 175 MPa.

The highest hardness belongs to the alloys containing Ca, followed by Sb, Bi, and RE.

The enhancement in creep resistance, shear strength, and hardness of the ternary alloys respect to the Mg-5Sn base alloy can be ascribed to their microstructural features. Introduction of alloying elements into the as-cast Mg-5Sn alloy leads to the formation of thermally stable phases and changes the morphology of Mg_2Sn particles. The respective melting points of Mg_3Bi_2, Mg_3Sb_2, and CaMgSn intermetallic compounds are 823, 1228, and 1184 °C, which are all higher than 771 °C for the Mg_2Sn phase. In addition, as shown in Fig. 3, the second phase particles lie in the interior parts of the dendrites as well as at the grain boundaries. Therefore, they can improve the strength of the grains, by obstructing the dislocation annihilation and thus restricting the slip inside the grains. On the other hand, presence of thermally stable phases at the grain boundaries results in inhibiting the grain boundary migration or grain boundary sliding during high-temperature plastic deformation [13]. The superior creep resistance, hardness, and shear strength of the Mg-5Sn-2Ca alloy is attributed to its refined microstructure and the higher volume fraction of the more thermally stable CaMgSn particles.

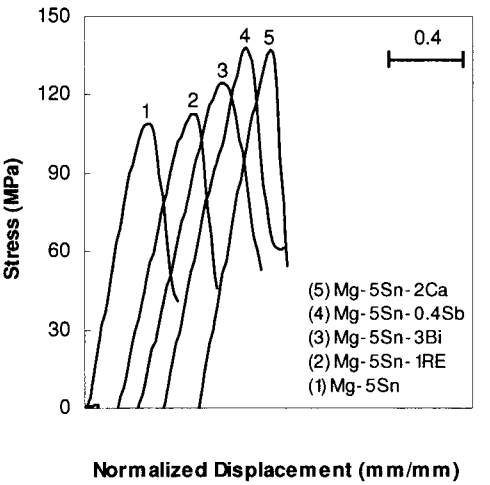

Fig. 5. Shear stress against normalized displacement for the tested materials.

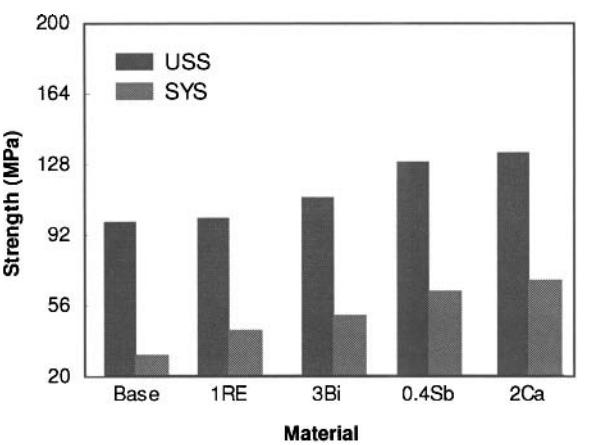

Fig. 6. Variation of USS and SYS values at room temperature for different materials in the as-cast conditions.

4. Conclusions

The microstructural evolution, creep resistance, hardness and room temperature shear strength of Mg-5Sn with additions of RE, Bi, Sb, and Ca were investigated in the as-cast condition. Microstructural analysis indicated that the addition of these elements refined the dendritic microstructure, modified the morphology of Mg_2Sn phase and caused the formation of some rod-shaped precipitates of Mg_3Bi_2, Mg_3Sb_2, and CaMgSn and branch-like RE-rich particles. These particles are all thermally stable phases, which strengthen both grains and grain boundaries and oppose both recovery and recrystallization processes during deformation processes at room and elevated temperatures, decreasing the minimum creep rate and increasing the hardness and strength of the material. The highest creep resistance, hardness, and shear strength of the Mg-5Sn-2Ca alloy is related to

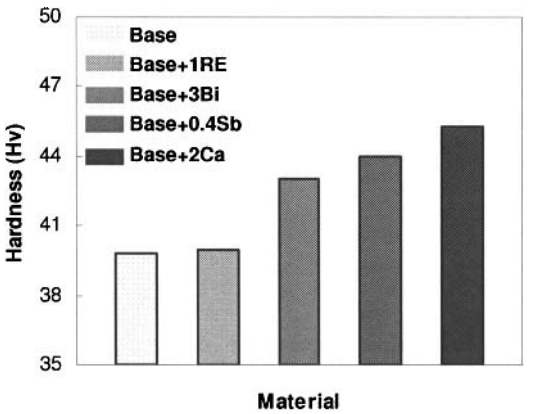

Fig. 7. Variation of hardness at room temperature for different materials in the as-cast conditions.

its refined microstructure and also to the higher volume fraction of the more thermally stable CaMgSn particles.

Reference

[1] B.L. Mordike, *J. Mater. Proc. Tech.*, 2001, 117, 391.

[2] B.L. Mordike, T. Ebert, Mater. Sci. Eng. A302 (2001) 37–45.

[3] N. Hort, Y. Huang, T.A. Leil, P. Maier, K.U. Kainer, Adv. Eng. Mater. 8 (2006) 359–364.

[4] G. Nayyeri, R. Mahmudi, Mater. Sci. Eng. A 527 (2010) 4613–4618.

[5] H. Liu, Y. Chen, Y. Tang, S. Wei, and G. Niu, *J. Alloys Compds.*, 2007, 440, 122.

[6] S. Wei, Y. Chen, Y. Tang, H. Liu, S. Xiao, G. Niu, X. Zhang, and Y. Zhao, *Mater. Sci. Eng. A,* 2008, 492, 20.

[7] G. Nayyeri, and R. Mahmudi, *Mater. Sci. Eng. A*, 2010, 527, 4613.

[8] G. Nayyeri, and R. Mahmudi, *Mater. Sci. Eng. A*, 2010, 527, 669.

[9] G. Nayyeri, and R. Mahmudi, *Mater. Sci. Eng. A*, 2010, 527, 2087.

[10] M. Keyvani, R. Mahmudi, and G. Nayyeri, *Mater. Sci. Eng. A,* doi: 10.1016/j.msea.2010.08.045.

[11] G. Nayyeri, and R. Mahmudi, *Mater. Sci. Eng. A*, 2010, 527, 5353.

[12] S. Wei, Y. Chen, Y. Tang, X. Zhang, M Liu, S. Xiao, and Y. Zhao, *Mater. Sci. Eng.*

[13] H. Liu, Y. Chen, Y. Tang, S. Wei, and G. Niu, *Mater. Sci. Eng. A*, 2007, 464, 124.

[14] R. Alizadeh, and R. Mahmudi, *Mater. Sci. Eng. A*, 2010, 527, 3975.

[15] R. Alizadeh, and R. Mahmudi, *Mater. Sci. Eng. A*, 2010, 527, 5312.

[16] R.K. Guduru, A.V. Nagasekhar, R.O. Scattergood, C.C. Koch, and K.L. Murty, *Metall. Mater. Trans.A,* 2006, 37, 1477.

[17] R. Mahmudi, A.R. Geranmayeh and A. Rezaee-Bazzaz, *Mater. Sci. Eng. A*, 2007, 448, 287.

[18] M. Bamberger, *Mater. Sci. Tech.*, 2001, 17, 15.